BIOCHEMISTRY
including biophysical chemistry & molecular biology

Rapid Report

pubs.acs.org/biochemistry

Crystal Structure of DNA Polymerase β with DNA Containing the Base Lesion Spiroiminodihydantoin in a Templating Position

Brian E. Eckenroth,[†] Aaron M. Fleming,[‡] Joann B. Sweasy,[§] Cynthia J. Burrows,[‡] and Sylvie Doublié*[,†]

[†]Department of Microbiology and Molecular Genetics, University of Vermont, Stafford Hall, 95 Carrigan Drive, Burlington, Vermont 05405, United States

[‡]Department of Chemistry, University of Utah, 315 South 1400 East, Salt Lake City, Utah 84112, United States

[§]Department of Therapeutic Radiology, Yale University School of Medicine, New Haven, Connecticut 06520, United States

Supporting Information

ABSTRACT: The first high-resolution crystal structure of spiroiminodihydantoin (dSp1) was obtained in the context of the DNA polymerase β active site and reveals two areas of significance. First, the structure verifies the recently determined *S* configuration at the spirocyclic carbon. Second, the distortion of the DNA duplex is similar to that of the single-oxidation product 8-oxoguanine. For both oxidized lesions, adaptation of the *syn* conformation results in similar backbone distortions in the DNA duplex. The resulting conformation positions the dSp1 A-ring as the base-pairing face whereas the B-ring of dSp1 protrudes into the major groove.

The DNA oxidation product deoxy-spiroiminodihydantoin (dSp) is produced via secondary oxidation of the common guanine damage 8-oxo-7,8-dihydroguanine (OG) along the reaction pathway that also produces guanidinohydantoin (Gh). Both dSp and Gh are excised by Nei-like glycosylases (NEILs) of the base excision repair pathway, with NEIL1 and NEIL3 removing these lesions in telomeric sequences.[1,2] When unrepaired, these oxidized bases can be highly mutagenic, with some replicative polymerases inserting either dATP or dGTP opposite the hydantoin lesions and others blocked at the lesion site.[3,4] The secondary oxidation event that converts OG to dSp produces an additional chiral center about the C4 position resulting in the conversion of the purine base into two perpendicularly oriented five-membered rings (Figure 1A), of which two diastereomers are possible: dSp1 and dSp2, recently reconciled as the *S* diastereomer and *R* diastereomer, respectively.[5,6] While several crystal structures of replicative DNA polymerases have been obtained with OG[7,8] or Gh[9,10] and with the DNA repair polymerase β (pol β) bound to OG-containing DNA,[11−13] no one so far has visualized the dSp lesion in the context of DNA.

Here we present the 2.08 Å crystal structure of DNA pol β variant E295K with dSp1 in the templating position, where dSp1 refers to the first diastereomer eluting from an ion-exchange column (Figure S1 of the Supporting Information). Crystals in the presence of the dSp1-containing single-nucleotide gapped DNA duplex were obtained as previously described.[14] The model was refined to a free *R* factor of 21.7% (R_{work} = 17.7%), root-mean-square deviations on bonds and angles of 0.002 Å and 0.66°, respectively, and a maximum likelihood coordinate error of 0.23 Å (Table 1). Attempts to crystallize wild-type (WT) pol β with the same oligonucleotide produced only small, poorly diffracting crystals. The E295K fingers domain variant serves as a viable model because the binary complex of the variant bound to DNA is isomorphous with that of the WT and the mutation does not negatively impact the binding affinity of the enzyme for DNA or the conformation of the templating base in the binary complex.[15] A similar approach was used to investigate lesion binding in the RB69 gp43 polymerase where the Y567A and L561A mutations were more amenable to structural studies involving Gh or *syn* OG.[8,10]

The crystal structure of the dSp1 pol β complex was obtained via isomorphous replacement by using an analogous complex containing dA in the templating position.[14] A composite omit map using a model devoid of dSp1 and neighboring nucleotides in the 3′ and 5′ direction was generated prior to model building (Figure 1B). Residual maps produced just prior to including the lesion revealed clear density verifying the lesion to be in the *syn* conformation. The maps also show clear density for water molecules within H-bonding distance of the base pairing face of the A-ring (Figure 1C).

Initial electron density maps suggested the orientation of the lesion represents the *S* diastereomer (dSp1). To verify the isomer of the dSp lesion within the DNA duplex, maps were calculated by substitution with the *R* diastereomer of dSp2 and evaluation of the electron density residual peaks (Figure 1D). The resulting strong peak/hole pair (greater than ±5σ) indicates that the position of N2 of the B-ring is consistent with the (*S*)-dSp configuration. A 3.0σ peak was also observed for the corresponding position of O6.

This binary structure sheds light on the implications for further oxidation of OG in the context of the DNA duplex: both OG and dSp1 generate distortions in the DNA backbone in the T(−1) and T(+1) positions (the nucleotide 5′ or 3′ to the templating position for the DNA polymerase). An isomorphous difference Fourier map (Figure 2A)[16] showed the clear position for the B-ring of (*S*)-dSp along with a rearrangement of the DNA backbone when compared to dA in the same position. The mean displacement for all backbone

Received: March 4, 2014
Revised: March 19, 2014
Published: March 20, 2014

   dx.doi.org/10.1021/bi500270e | *Biochemistry* 2014, 53, 2075−2077

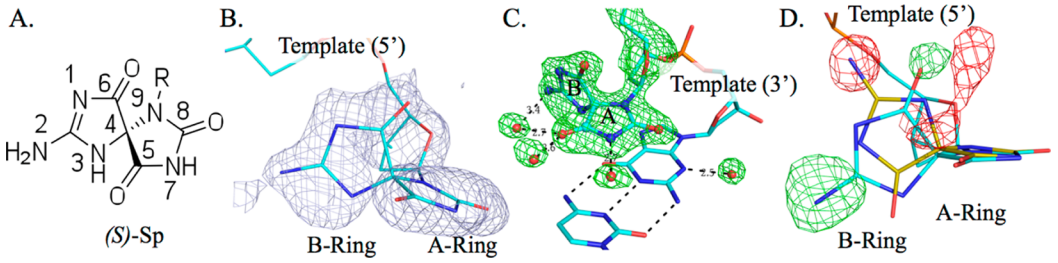

Figure 1. Verification of the *S* diastereomer configuration of dSp. (A) Drawing of (*S*)-Sp, with the numbering based on guanine. (B) Composite omit map (gray mesh) contoured at 1.2σ of dSp. (C) Residual map (green mesh, 3σ) prior to inclusion of the lesion in the model. (D) Residual map (green for +3σ and red for −3σ) calculated with the *R* diastereomer colored beige with a superposition of the *S* diastereomer (cyan), illustrating that dSp1 adopts the *S* configuration.

Table 1. Crystallographic Data Collection and Refinement

PDB entry	4PPX
space group	*P*2(1)
cell dimensions	a = 54.3 Å, b = 79.1 Å, c = 54.7 Å, β = 105.4°
resolution (Å)	14−2.08 (2.15−2.08)[a]
no. of unique reflections	25842
completeness (%)	96.4 (80.7)
redundancy	3.3 (2.2)
R_{merge} (%)[b]	5.0 (26.1)
I/σ	22.8 (3.4)
Wilson *B* factor (Å^2)	27.0
Refinement	
R_{work}/R_{free} (%)	17.7 (21.7)
rmsd[c] for bonds (Å)	0.002
rmsd[c] for angles (deg)	0.66
coordinate error, maximum likelihood (Å)	0.23
B factor (Å^2)	
protein	35.3
DNA	33.0
sodium ion	27.9
water	38.4
no. of atoms	
protein	2472
DNA	630
sodium ion	2
water	348

[a]Values in parentheses denote data for the highest-resolution shell. [b]$R_{merge} = (\sum|I_i - \langle I\rangle|)/\sum|I|$, where $\langle I\rangle$ is the mean intensity of measured observations for reflection I_i. [c]Root-mean-square deviation.

atoms, including N9, is 1.9 Å, with the largest being for the 5′-PO_4 atom of the lesion with displacements of 2.4 and 2.3 Å for the 3′-hydroxyl. The distortion is most notable for the changes in both the α (from 64° to −65°) and γ (from 55° to −90°) torsion angles for the dSp position. These angles are unchanged regardless of whether the comparison involves the WT or the E295K binary complex with undamaged DNA. A summary of the torsion angles for T(−1), the lesion, and T(+1) is listed in Table S1 of the Supporting Information for comparison with those of the pol β E295K variant containing dA and the WT containing a templating dG. Interestingly, the 5′-PO_4 repositioning matches that seen for the *syn* OG in the active site of WT pol β (Figure 2B).[12] A comparison with WT pol β and templating dG is shown in Figure S2 of the Supporting Information.

Molecular dynamics simulation calculations predicted (*R*)-dSp to favor the *anti* form and (*S*)-dSp to favor the *syn* form in

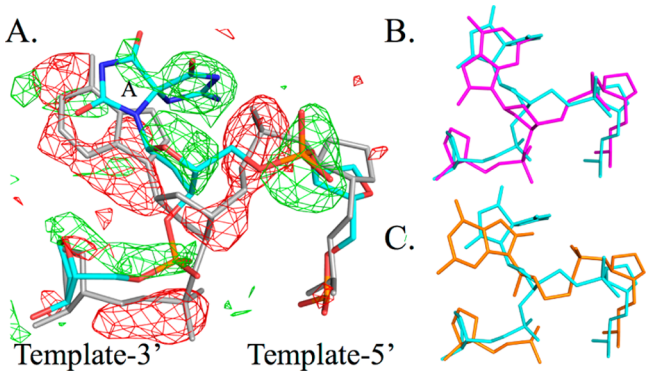

Figure 2. Backbone distortion of the (*S*)-Sp-containing DNA strand. (A) $F_o - F_o$ isomorphous difference Fourier map (±3σ) between dA (gray) and (*S*)-dSp (cyan) in the templating position. The (*S*)-dSp A-ring is indicated. (B and C) (*S*)-dSp DNA (cyan) in comparison with OG[12] (Protein Data Bank entry 3RJE) (B) in the *syn* conformation (magenta) or (C) in the *anti* conformation (orange) (same orientation as panel A).

the interior context of a DNA duplex.[17] In the dSp1 pol β structure, a collection of clashes requires dSp1 to adopt the predicted *syn* conformation in the DNA duplex. Placement of the B-ring in the *anti* position on the minor groove side of the duplex would place O6 of the lesion 1.1 Å from the purine ring of the T(−1) position. There would also be a clash of N2 with the OH of Tyr271 (1.8 Å) in the polymerase active site (Figure S3A of the Supporting Information). Selection of the *syn* conformation due to these clashes dictates the backbone distortion for the T(+1) position with the repositioning of the B-ring to the major groove side. Prior to backbone rearrangement, the nonbridging oxygens of the phosphodiester linkage between T(+1) and the lesion would be 1.4 Å from N1 and 2.1 Å from C6 of the B-ring (Figure S3B of the Supporting Information).

Crystals were subsequently soaked with a deoxynucleoside triphosphate, either dCTP, dATP, dGTP, or the non-hydrolyzable analogue 2′-deoxyuridine 5′-(α,β)-imidotriphosphate (dUMPNPP), in the attempt to capture a ternary complex. X-ray data were collected on all four types of soaked crystals, but none of the crystals resulted in the formation of a ternary complex with visible density for the incoming nucleotide, which is consistent with the low Cross *R* values ranging from 18 to 26% on intensity comparing the putative ternary complexes with the binary form. The most significant density in the isomorphous difference Fourier maps was for that of the dUMPNPP triphosphate and ribose moiety. However, the conformational change in the fingers domain

dx.doi.org/10.1021/bi500270e | *Biochemistry* 2014, 53, 2075−2077

expected upon nucleotide binding was not observed for any of the soaks. The resulting poor binding could be due to the lesion itself or the nucleotide binding properties of E295K.[14] An additional mutation akin to the Y567A variant in RB69 gp43, which opened the polymerase active site and was necessary to visualize a Gh−dATP ternary complex,[10] may be necessary to capture a ternary complex with pol β bound to (*S*)-dSp-containing DNA and dNTP.

■ ASSOCIATED CONTENT

Supporting Information

A description of materials and methods along with Figures S1−S3 and Table S1. This material is available free of charge via the Internet at http://pubs.acs.org.

Accession Codes

The coordinates and structure factors have been deposited as Protein Data Bank entry 4PPX.

■ AUTHOR INFORMATION

Corresponding Author

*E-mail: sdoublie@uvm.edu. Telephone: (802) 656-9531.

Funding

These studies were funded by National Institutes of Health Grants R01 CA080830 to J.B.S., R01 CA090689 to C.J.B., and R01 CA052040 to S.D.

Notes

The authors declare no competing financial interest.

■ ACKNOWLEDGMENTS

We thank April Averill for protein purification and Haein Kim for help with crystallization trials.

■ REFERENCES

(1) Zhao, X., Krishnamurthy, N., Burrows, C. J., and David, S. S. (2010) Mutation versus repair: NEIL1 removal of hydantoin lesions in single-stranded, bulge, bubble, and duplex DNA contexts. *Biochemistry 49*, 1658−1666.

(2) Zhou, J., Liu, M., Fleming, A. M., Burrows, C. J., and Wallace, S. S. (2013) Neil3 and NEIL1 DNA glycosylases remove oxidative damages from quadruplex DNA and exhibit preferences for lesions in the telomeric sequence context. *J. Biol. Chem. 288*, 27263−27272.

(3) Henderson, P. T., Delaney, J. C., Muller, J. G., Neeley, W. L., Tannenbaum, S. R., Burrows, C. J., and Essigmann, J. M. (2003) The hydantoin lesions formed from oxidation of 7,8-dihydro-8-oxoguanine are potent sources of replication errors in vivo. *Biochemistry 42*, 9257−9262.

(4) Kornyushyna, O., and Burrows, C. J. (2003) Effect of the oxidized guanosine lesions spiroiminodihydantoin and guanidinohydantoin on proofreading by *Escherichia coli* DNA polymerase I (Klenow fragment) in different sequence contexts. *Biochemistry 42*, 13008−13018.

(5) Fleming, A. M., Orendt, A. M., He, Y., Zhu, J., Dukor, R. K., and Burrows, C. J. (2013) Reconciliation of chemical, enzymatic, spectroscopic and computational data to assign the absolute configuration of the DNA base lesion spiroiminodihydantoin. *J. Am. Chem. Soc. 135*, 18191−18204.

(6) Ding, S., Jia, L., Durandin, A., Crean, C., Kolbanovskiy, A., Shafirovich, V., Broyde, S., and Geacintov, N. E. (2009) Absolute configurations of spiroiminodihydantoin and allantoin stereoisomers: Comparison of computed and measured electronic circular dichroism spectra. *Chem. Res. Toxicol. 22*, 1189−1193.

(7) Brieba, L. G., Eichman, B. F., Kokoska, R. J., Doublié, S., Kunkel, T. A., and Ellenberger, T. (2004) Structural basis for the dual coding potential of 8-oxoguanosine by a high-fidelity DNA polymerase. *EMBO J. 23*, 3452−3461.

(8) Hogg, M., Rudnicki, J., Midkiff, J., Reha-Krantz, L., Doublié, S., and Wallace, S. S. (2010) Kinetics of mismatch formation opposite lesions by the replicative DNA polymerase from bacteriophage RB69. *Biochemistry 49*, 2317−2325.

(9) Aller, P., Ye, Y., Wallace, S. S., Burrows, C. J., and Doublié, S. (2010) Crystal structure of a replicative DNA polymerase bound to the oxidized guanine lesion guanidinohydantoin. *Biochemistry 49*, 2502−2509.

(10) Beckman, J., Wang, M., Blaha, G., Wang, J., and Konigsberg, W. H. (2010) Substitution of Ala for Tyr567 in RB69 DNA polymerase allows dAMP and dGMP to be inserted opposite guanidinohydantoin. *Biochemistry 49*, 8554−8563.

(11) Krahn, J. M., Beard, W. A., Miller, H., Grollman, A. P., and Wilson, S. H. (2003) Structure of DNA polymerase β with the mutagenic DNA lesion 8-oxodeoxyguanine reveals structural insights into its coding potential. *Structure 11*, 121−127.

(12) Batra, V. K., Shock, D. D., Beard, W. A., McKenna, C. E., and Wilson, S. H. (2012) Binary complex crystal structure of DNA polymerase β reveals multiple conformations of the templating 8-oxoguanine lesion. *Proc. Natl. Acad. Sci. U.S.A. 109*, 113−118.

(13) Freudenthal, B. D., Beard, W. A., and Wilson, S. H. (2013) DNA polymerase minor groove interactions modulate mutagenic bypass of a templating 8-oxoguanine lesion. *Nucleic Acids Res. 41*, 1848−1858.

(14) Eckenroth, B. E., Towle-Weicksel, J. B., Sweasy, J. B., and Doublié, S. (2013) The E295K cancer variant of human polymerase β favors the mismatch conformational pathway during nucleotide selection. *J. Biol. Chem. 288*, 34850−34860.

(15) Lang, T., Dalal, S., Chikova, A., DiMaio, D., and Sweasy, J. B. (2007) The E295K DNA polymerase β gastric cancer-associated variant interferes with base excision repair and induces cellular transformation. *Mol. Cell. Biol. 27*, 5587−5596.

(16) Rould, M. A., and Carter, C. W., Jr. (2003) Isomorphous difference methods. *Methods Enzymol. 374*, 145−163.

(17) Jia, L., Shafirovich, V., Shapiro, R., Geacintov, N. E., and Broyde, S. (2005) Spiroiminodihydantoin lesions derived from guanine oxidation: Structures, energetics, and functional implications. *Biochemistry 44*, 6043−6051.